Physics reach of the ESSnuSB experiment

Monojit Ghosh[1]

Center of Excellence for Advanced Materials and Sensing Devices, Ruder Bošković Institute, 10000 Zagreb, Croatia
School of Physics, University of Hyderabad, Hyderabad - 500046, India

E-mail: monojit_rfp@uohyd.ac.in

Abstract. ESSnuSB is a unique future proposed long-baseline experiment in Sweden to study neutrino oscillation by probing the second oscillation maximum. In this proceeding, we update the flux and efficiencies and re-calculate the sensitivity of ESSnuSB in the standard three flavour scenario. We find that it has excellent sensitivity to the Dirac CP phase $\delta_{\rm CP}$, moderate sensitivity to the mass hierarchy of the neutrinos and limited sensitivity to measure the octant of the atmospheric mixing angle θ_{23}. We also find that it has a very good sensitivity to constrain the atmospheric mass squared difference $|\Delta m^2_{31}|$.

1. Introduction

Among the six parameters (θ_{12}, θ_{13}, θ_{23}, Δm^2_{21}, Δm^2_{31} and $\delta_{\rm CP}$) that describe the neutrino oscillation in standard three flavour scenario, the current unknowns are: (i) neutrino mass hierarchy which can be either normal i.e.,$\Delta m^2_{31} < 0$ or inverted i.e., $\Delta m^2_{31} < 0$, (ii) the octant of θ_{23} which can be either higher i.e., $\theta_{23} > 45^\circ$ or lower i.e., $\theta_{23} < 45^\circ$ and (iii) $\delta_{\rm CP}$ [1]. ESSnuSB [2, 3, 4] is one of the proposed long-baseline experiments in Sweden which aims to measure the CP phase $\delta_{\rm CP}$ by probing the second oscillation maximum. As the variation of the oscillation probability with respect to $\delta_{\rm CP}$ is higher in the second oscillation maximum as compared to the first oscillation maximum, this experiment can measure $\delta_{\rm CP}$ with very good precision.

In this proceedings, we have updated the calculation of flux and efficiencies and re-calculated the sensitivity of ESSnuSB to measure the unknowns mentioned above in the standard three flavour scenario. This proceedings is organized as follows. In the next section we will give the details of the simulation which we used in our calculation. Then we will present our results. Finally we will summarize and conclude.

2. Simulation Details

We consider a water Cherenkov detector of fiducial volume 538 kt located either at a distance of 540 km or 360 km from the neutrino source. Neutrino beam is produced by a powerful linear accelerator (linac) capable of delivering 2.7×10^{23} protons on target per year having a beam power of 5 MW with proton kinetic energy of 2.5 GeV. The fluxes and the event selection for the Far Detectors are estimated using full Monte Carlo simulations specific to the ESSnuSB conditions. These fluxes and detector response with efficiencies are then incorporated in GLoBES [5, 6] to calculate event rates and χ^2. We have considered the systematic errors on the overall

[1] On behalf of the ESSnuSB collaboration

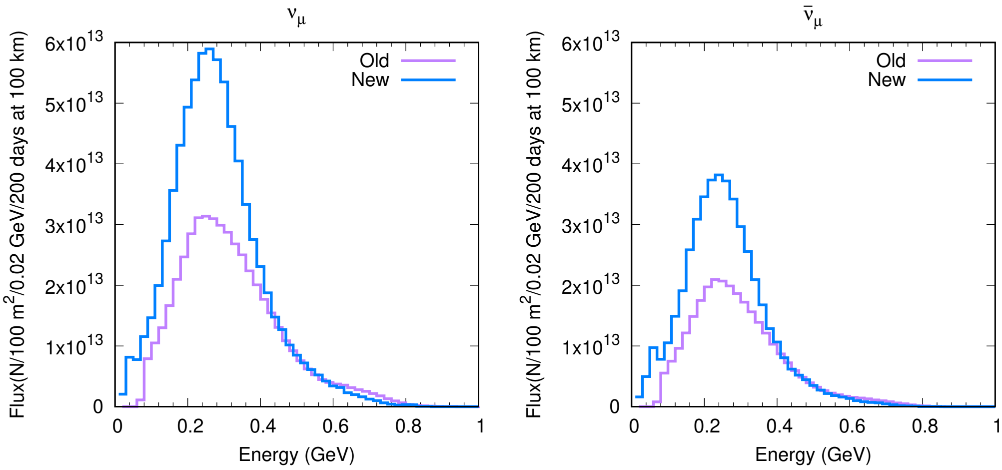

Figure 1. Neutrino fluxes as a function of energy. The left panel is for positive polarity and the right panel is for negative polarity.

normalization of the expected number of detected events at the Far Detectors: 5% for signal and 10% for background. No systematic effects on the shape of the detected energy spectrum have been implemented. The systematic errors are considered to be the same for appearance and disappearance channels for both neutrinos and antineutrinos. We have considered a total run-time of 10 years which is divided into 5 years of neutrino beam and 5 years of antineutrino beam. The configurations are same for both baseline options of ESSnuSB.

3. Results

In Fig. 1, we have presented the muon flux as a function of energy. The left panel is for positive polarity and the right panel is for negative polarity. In each panel the purple curve corresponds to the old flux as given in [7] and the blue curve corresponds to the updated flux used in this analysis. From this panel we understand that there is a significant improvement in the updated flux.

In Fig. 2, we have plotted the efficiency as a function true energy. The left column is for the previous selection as given in [7] and the right column is for the updated selection which is used in the present calculation. From these panels we understand that the updated ν_e signal efficiency (purple curve in the top row) is much higher as compared to the previous selection, whereas the updated ν_μ efficiency (purple curve in the bottom row) is somewhat similar to the previous selection. As CP sensitivity mainly comes from the appearance channel, we expect a significant improvement in the CP sensitivity with the current selection.

In Fig. 3, we have plotted the CP sensitivity of ESSnuSB with the updated flux and updated efficiencies. The left panel is for CP violation and the right panel is for CP precision. In each panel, the purple curve corresponds to 540 km and the red curve corresponds to 360 km. For CP violation, we understand that for $\delta_{CP} = \pm 90^\circ$, we have around 14σ sensitivity for 360 km baseline and around 10σ sensitivity for 540 km baseline. For CP precision, we understand that the 1σ precision of $\delta_{\rm CP}$ is around 5° if the true values of $\delta_{\rm CP}$ are around 0° or 180° for both baseline options. However, for $\delta_{\rm CP} = -90^\circ$, the error is around 14° for the baseline option of 540 km and only 7° for the baseline option of 360 km. CP sensitivity for 360 km is higher because of the larger statistics at the smaller baseline.

In Fig. 4, we present the hierarchy and octant sensitivity of ESSnuSB. In the left panel we present the hierarchy sensitivity as a function of $\delta_{\rm CP}$ (true). The purple curve corresponds to the

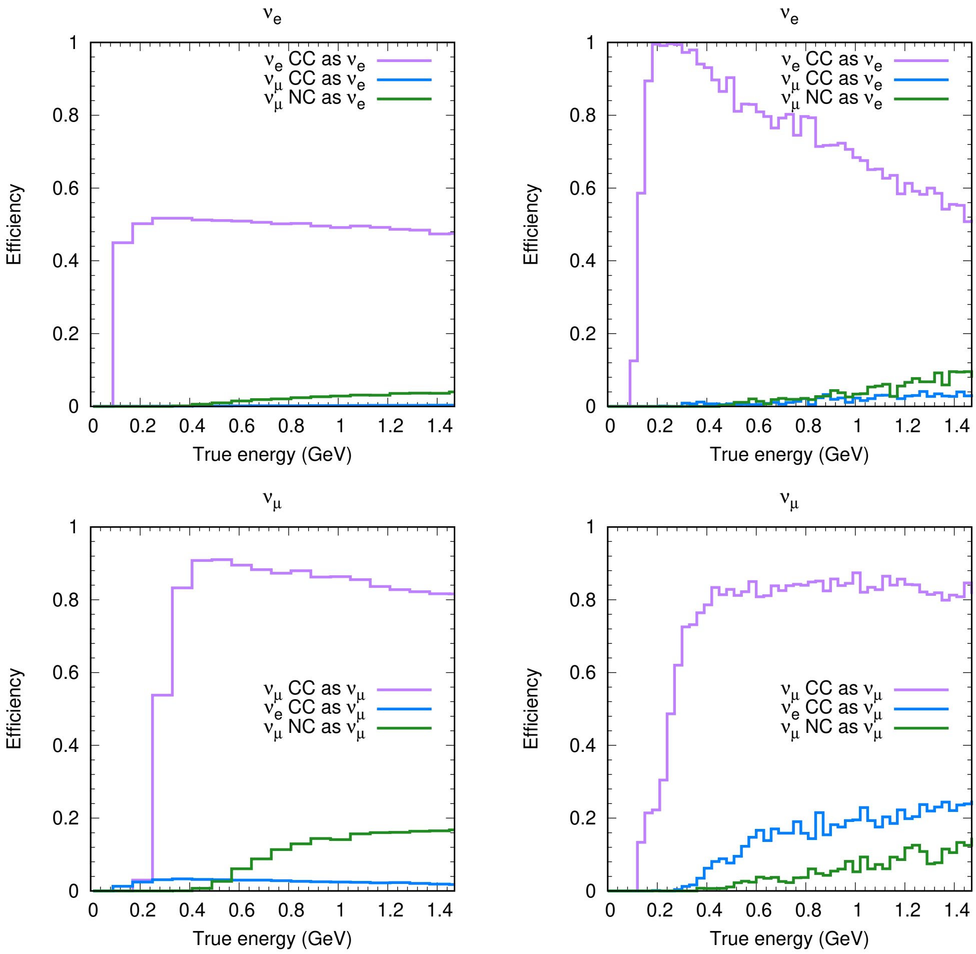

Figure 2. Efficiencies as a function of energy. The left column is for previous selection and the right column is for updated selection.

baseline option of 540 km and the red curve corresponds to the baseline option of 360 km. The black horizontal lines correspond to the benchmark of 3σ and 5σ sensitivity, respectively. From this panel we understand that for the baseline option of 540 km, one can have a 3σ hierarchy sensitivity except for $\delta_{\rm CP} = \pm 90^\circ$, and for the baseline option of 360 km one can have a hierarchy sensitivity of 5σ for all the values of $\delta_{\rm CP}$. The hierarchy sensitivity is higher for 360 km is because of higher matter effect. In the middle and left panels we present the octant sensitivity in the θ_{23} (true) vs $\delta_{\rm CP}$ (true) plane. The middle panel is for the baseline option of 540 km and the right panel is for the baseline option of 360 km. In each panel the purple/red/blue curve corresponds to the $1\sigma/2\sigma/3\sigma$ contours, respectively. In these panels, the region around $\theta_{23} = 45^\circ$ shows the values of θ_{23} for which the octant cannot be determined at that given C.L. From these panels we see that the octant sensitivity of ESSnuSB is limited. In these panels the sensitivity of 360 km is slightly better than the 540 km.

Finally, in Fig. 5, we plot the precision measurement of the atmospheric mixing parameters of ESSnuSB in the θ_{23} (test) - Δm^2_{31} (test) plane. The left panel is for the baseline option of 540 km and the right panel is for the baseline option of 360 km. In each panel, the purple/red/blue curve corresponds to the $1\sigma/2\sigma/3\sigma$ C.L. contours, respectively. The measured central values of θ_{23} and Δm^2_{31} are indicated by a star. From these panels we understand that the capability

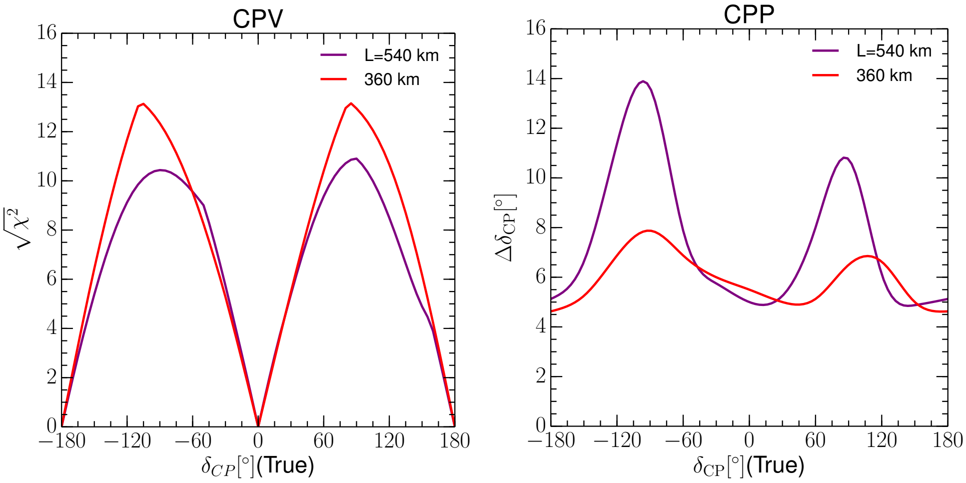

Figure 3. CP violation sensitivity (left panel) and CP precision sensitivity (right panel) as a function of δ_{CP} true.

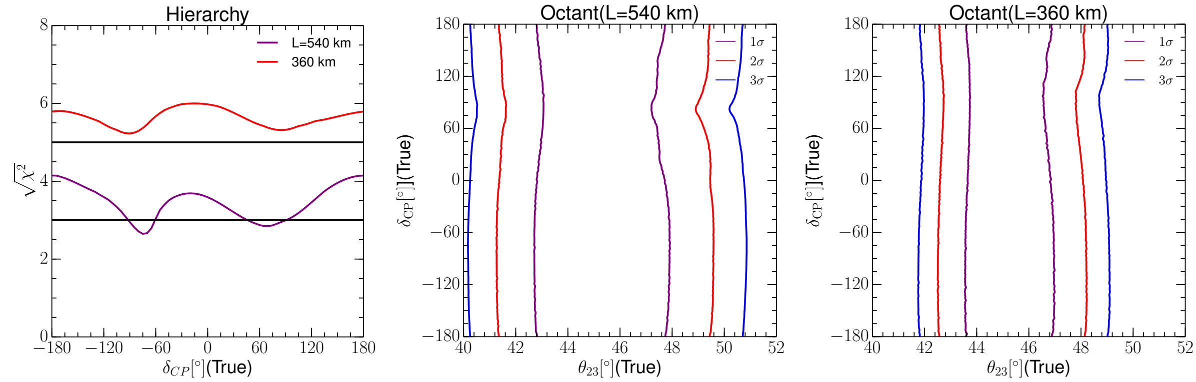

Figure 4. Hierarchy sensitivity (left panel) as a function of δ_{CP} true and octant sensitivity (middle and left panel) in the θ_{23} true - δ_{CP} true plane.

of ESSnuSB to constrain Δm^2_{31} is quite good, while its capability to constrain θ_{23} is limited. In terms of the precision of the atmospheric mixing parameters, the capability of the 360 km baseline is significantly better than the 540 km baseline.

We have generated all the figures for normal mass hierarchy of the neutrinos. The true value of the oscillation parameters are: $\theta_{12} = 33.44°$, $\theta_{13} = 8.57°$, $\theta_{23} = 49.2°$, $\Delta m^2_{21} = 7.42 \times 10^{-5}$ eV^2, $\Delta m^2_{31} = 2.517 \times 10^{-3}$ eV2 and $\delta_{CP} = -163°$. We have minimzed the parameters θ_{23} and δ_{CP} in the test spectrum of the χ^2.

4. Summary and Conclusion

In this proceeding, we have studied the physics reach of the ESSnuSB experiment in the standard three flavour scenario, with the updated flux and updated selection. We have shown that the current updated flux are significantly better than the previous flux. Whereas the current ν_e event selection is much better than the previous ν_e selection but the current ν_μ selection is comparable with the previous selection. In our analysis we find that, CP violation discovery

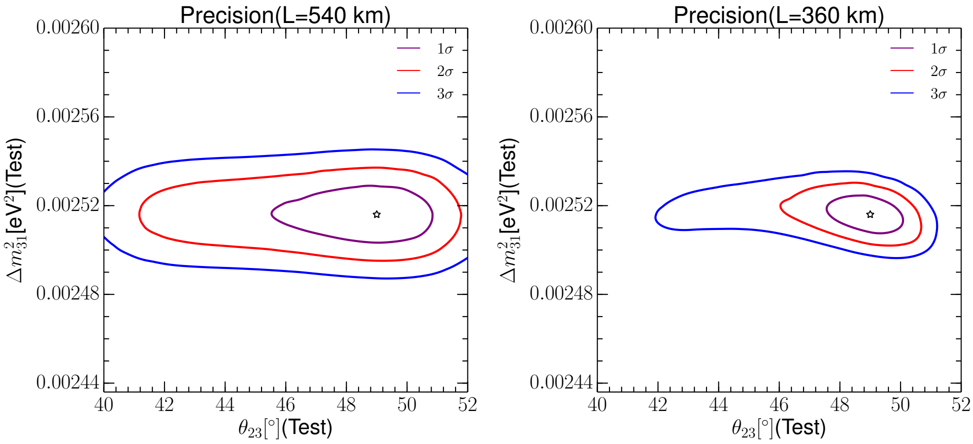

Figure 5. Precision of the atmospheric mixing parameters. Left panel is for 540 km and the right panel is for 360 km.

sensitivity is 10σ (13σ) for the baseline option of 540 km (360 km) at $\delta_{\rm CP} = \pm 90°$. Regarding CP precision, the 1σ error associated with $\delta_{\rm CP} = 0°$ is around 5° for both of the baseline options and the error associated with $\delta_{\rm CP} = -90°$ is around 14° (7°) for the baseline option of 540 km (360 km). For neutrino mass hierarchy, one can achieve 3σ sensitivity for the 540 km baseline except for the true values of $\delta_{\rm CP} = \pm 90°$ and 5σ sensitivity for the 360 km baseline for all values of $\delta_{\rm CP}$. The values of θ_{23} for which the octant can be determined at 3σ is $\theta_{23} > 51°$ ($\theta_{23} < 42°$ and $\theta_{23} > 49°$) for the baseline of 540 km (360 km). Regarding the precision of the atmospheric mixing parameters, the allowed values at 3σ are: $40° < \theta_{23} < 52°$ ($42° < \theta_{23} < 51.5°$) and 2.485×10^{-3} eV$^2 < \Delta m^2_{31} < 2.545 \times 10^{-3}$ eV^2 (2.49×10^{-3} eV$^2 < \Delta m^2_{31} < 2.54 \times 10^{-3}$ eV^2) for the baseline of 540 km (360 km). Among the two baseline options, 360 km provides the better sensitivity. For more details see Ref. [8] on which this proceeding is based upon.

Acknowledements
This project received funding from the European Union's Horizon 2020 research and innovation programme under grant agreement No. 777419. This is also partly funded by Ramanujan Fellowship of SERB, Govt. of India, through grant no: RJF/2020/000082.

References
[1] I. Esteban, M. C. Gonzalez-Garcia, M. Maltoni, T. Schwetz and A. Zhou, JHEP **09**, 178 (2020) [arXiv:2007.14792 [hep-ph]].
[2] E. Baussan *et al.* [ESSnuSB], Nucl. Phys. B **885**, 127-149 (2014) [arXiv:1309.7022 [hep-ex]].
[3] E. Wildner, E. Baussan, M. Blennow, M. Bogomilov, A. Burgman, E. Bouquerel, C. Carlile, J. Cederkäll, P. Christiansen and P. Cupial, *et al.* Adv. High Energy Phys. **2016**, 8640493 (2016) [arXiv:1510.00493 [physics.ins-det]].
[4] M. Blennow, E. Fernandez-Martinez, T. Ota and S. Rosauro-Alcaraz, Eur. Phys. J. C **80**, 190 (2020) [arXiv:1912.04309 [hep-ph]].
[5] P. Huber, M. Lindner and W. Winter, Comput. Phys. Commun. **167**, 195 (2005) [arXiv:hep-ph/0407333 [hep-ph]].
[6] P. Huber, J. Kopp, M. Lindner, M. Rolinec and W. Winter, Comput. Phys. Commun. **177**, 432-438 (2007) [arXiv:hep-ph/0701187 [hep-ph]].
[7] L. Agostino *et al.* [MEMPHYS], JCAP **01**, 024 (2013) [arXiv:1206.6665 [hep-ex]].
[8] A. Alekou *et al.* [ESSnuSB], [arXiv:2107.07585 [hep-ex]].